

## Synthesis of Ferric Oxide Nanoparticles with Controllable Crystal Phases by Salt-assisted Combustion Method

SONG Jun<sup>1</sup>, MA Zhen-Ye<sup>1,2</sup>, LI Cheng<sup>1</sup>, WU Ru-Jun<sup>2</sup>

(1. State Key Laboratory of Materials-Oriented Chemical Engineering, Nanjing University of Technology, Nanjing 210009, China,  
2. College of Chemistry and Environment Science, Nanjing Normal University, Nanjing 210097, China)

**Abstract:** The salt-assisted combustion method was applied in synthesis of  $\text{Fe}_2\text{O}_3$  nanoparticles by using  $\text{Fe}(\text{NO}_3)_3 \cdot 9\text{H}_2\text{O}$ , polyethylene glycol (PEG2000) and KCl as oxidant, fuel and salt, respectively. The products were characterized by HRTEM, XRD, LRS and  $\text{N}_2$  adsorption. It is found that the crystal phase (including  $\alpha\text{-Fe}_2\text{O}_3$ ,  $\gamma\text{-Fe}_2\text{O}_3$  and the mixed phases of  $\alpha\text{-Fe}_2\text{O}_3$  and  $\gamma\text{-Fe}_2\text{O}_3$ ) of  $\text{Fe}_2\text{O}_3$  nanoparticles can be adjusted by changing the  $\text{KCl}/\text{NO}_3^-$  molar ratio. Addition of soluble inert KCl in the redox mixture solution for combustion synthesis results in the formation of well-dispersed  $\gamma\text{-Fe}_2\text{O}_3$  nanoparticles and a drastic increase in the specific surface area from 21.96 to 102.35  $\text{m}^2/\text{g}$ . A mechanism was proposed to illustrate the possible formation process of different crystal phase nanoparticles with different character.

**Key words:**  $\text{Fe}_2\text{O}_3$  nanoparticles; salt-assisted combustion; crystal phase

Nanometer-sized ferric oxide ( $\text{Fe}_2\text{O}_3$ ) is widely used in many fields including pigments, catalysts, ceramics and magnetic recording materials. During the past two decades, considerable attention has been paid to preparation of  $\text{Fe}_2\text{O}_3$  with different sizes, morphologies and crystal phases<sup>[1]</sup>. For this purpose, some methods, including Sol-Gel method<sup>[2-9]</sup>, forced hydrolysis method<sup>[10-13]</sup>, hydrothermal method<sup>[14-18]</sup>, oil-water two phase method<sup>[19]</sup> and combustion method were thus developed<sup>[20]</sup>. Among them, the combustion method has attracted considerable interest due to its excellent advantages such as simple process, low cost, short time, little energy consumption and high production yield<sup>[21-22]</sup>. This process utilizes the exothermicity of the redox reaction between oxidizer and fuel to directly crystallize the materials from the molecular mixture of precursor solutions. However, it is hard to obtain well-dispersed nanoparticles because of their aggregation in combustion process. To overcome this shortcoming, a novel salt-assisted combustion method (SACM) was developed and successfully applied in preparation of well dispersed various oxides and

composite oxides nanoparticles<sup>[23-26]</sup>. To the best of our knowledge, this method has not been used in preparation of  $\text{Fe}_2\text{O}_3$  nanoparticles.

In this paper, the SACM was introduced to  $\text{Fe}_2\text{O}_3$  nanoparticle preparation by using  $\text{Fe}(\text{NO}_3)_3 \cdot 9\text{H}_2\text{O}$ , polyethylene glycol (PEG2000) and KCl as oxidizer, fuel and salt respectively. Efforts were focused on crystal-phase and micro-structure control of  $\text{Fe}_2\text{O}_3$  nanoparticles. The resulting products were characterized by HRTEM, XRD, LRS and  $\text{N}_2$  adsorption.

## 1 Experiment

$\text{Fe}(\text{NO}_3)_3 \cdot 9\text{H}_2\text{O}$ , poly ethylene glycol (PEG2000) and kalium chloride (KCl) were analytical grade. Double distilled water was used in preparation.

The preparation procedure was as follow: First, 0.006 mol  $\text{Fe}(\text{NO}_3)_3 \cdot 9\text{H}_2\text{O}$  was dissolved in 100 mL aqueous solution of PEG2000 with a  $\text{NO}_3^-/\text{PEG2000}$  molar ratio of 1. Then, the desired amount of KCl was added to the

Received date: 2009-12-20, Modified date: 2010-03-02, Published online: 2010-03-20

Foundation item: National Natural Science Foundation of China (50702025); Natural Science Foundation of Jiangsu province (BK2009473); Natural Science Foundation of the Jiangsu Higher Education Institutions of China (08KJB430009); Youth Foundation of Nanjing University of Technology (39071014); Foundation of State Key Laboratory of Materials-Oriented Chemical Engineering (KL09-13)

Biography: SONG Jun(1973—), female, PhD candidate, lecturer. E-mail: sj7366@njut.edu.cn

Corresponding author: MA Zhen-Ye, associate professor. E-mail: 07197@njnu.edu.cn

above solution and the resulting transparent solution was thoroughly stirred by a magnetic mixer at 70 °C until a homogeneous sol-like solution was formed. Afterwards, the sol-like solution was dried at 110 °C for 2 h. The obtained gel was placed in a silica crucible and heated in air until the gel was ignited. The as-burned powders were boiled in deionized water to remove the salt. Final products were obtained after filtrating, washing with deionized water and ethanol, drying at 80 °C for 2 h.

For comparison, Fe<sub>2</sub>O<sub>3</sub> samples were also prepared in the absence of KCl with the similar procedure which was denoted as S1. Samples prepared with KCl/NO<sub>3</sub><sup>-</sup> molar ratios of 1:2, 1:1, 2:1 and 4:1, were denoted as S2, S3, S4 and S5 respectively. The products were characterized with high resolution transmission electron microscope (HRTEM, JEOL JEM-2100), X-ray diffraction using Cuka (XRD, Bruker D8 Advance), Laser Raman spectroscopy (LRS, Renishaw invia), N<sub>2</sub> adsorption (Bechman Coulter SA3100 Plus) and thermogravimetric and differential thermal analysis (TG-DTA, Perkin-Elmer Diamond) with a heating rate of 20 °C/min in N<sub>2</sub>.

## 2 Results and discussion

Figure 1 shows XRD patterns of the Fe<sub>2</sub>O<sub>3</sub> nanoparticles S1-S5. S1 (Fig. 1 (a)) can be exclusively indexed to  $\alpha$ -Fe<sub>2</sub>O<sub>3</sub> without impurity according to standard data (JCPDS 33-0664). The diffraction peaks of XRD patterns of S2 and S3 (Fig. 1 (b) and (c)) can be well assigned to a spinel structure with the characteristic diffraction of  $\gamma$ -Fe<sub>2</sub>O<sub>3</sub> (JCPDS 39-1346) or Fe<sub>3</sub>O<sub>4</sub> (JCPDS 19-0629). In order to certify samples S2 and S3 clearly, LRS characterization was conducted. Figure 2 shows the LRS of samples S3, which exhibits three peaks at 700, 500 and 350 cm<sup>-1</sup>, corresponding to the different characteristic bands of  $\gamma$ -Fe<sub>2</sub>O<sub>3</sub><sup>[27]</sup>. Consequently, it should be reasonable to postulate that samples S2 and S3 are  $\gamma$ -Fe<sub>2</sub>O<sub>3</sub>. From Fig. 1 (a) and Fig. 1 (c), it can be seen that S3 shows a more perfect phase than S1 due to the narrower diffraction peaks, which may be explained by the fact that the melt salt is capable of accelerating the material formation kinetics and improving the product crystallinity<sup>[28]</sup>. The diffraction peaks of S4 and S5, shown in Fig. 1 (d) and 1 (e), correspond to the characteristic peaks of both  $\alpha$ -Fe<sub>2</sub>O<sub>3</sub> and  $\gamma$ -Fe<sub>2</sub>O<sub>3</sub>, indicating that the Fe<sub>2</sub>O<sub>3</sub> samples are a mixture of  $\alpha$ -Fe<sub>2</sub>O<sub>3</sub> and  $\gamma$ -Fe<sub>2</sub>O<sub>3</sub>. Above results show that crystal-phase of Fe<sub>2</sub>O<sub>3</sub> nanoparticles (including pure  $\alpha$ -Fe<sub>2</sub>O<sub>3</sub>, pure  $\gamma$ -Fe<sub>2</sub>O<sub>3</sub> and the mixture phase of  $\alpha$ -Fe<sub>2</sub>O<sub>3</sub> and  $\gamma$ -Fe<sub>2</sub>O<sub>3</sub>) can be adjusted by changing the molar ratio of KCl/NO<sub>3</sub><sup>-</sup>. However, the combustion reaction couldn't occur when the KCl/NO<sub>3</sub><sup>-</sup> molar ratio exceeded 6:1.

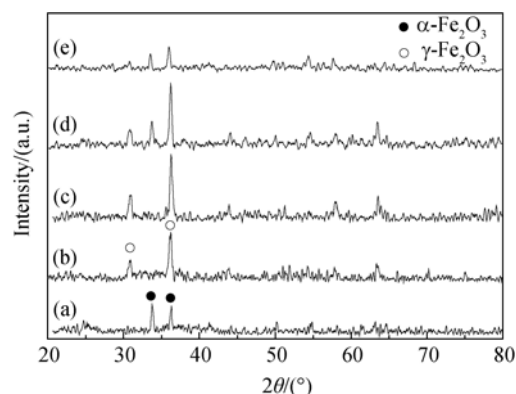


Fig. 1 XRD patterns of different Fe<sub>2</sub>O<sub>3</sub> samples (a) S1, (b) S2, (c) S3, (d) S4, (e) S5

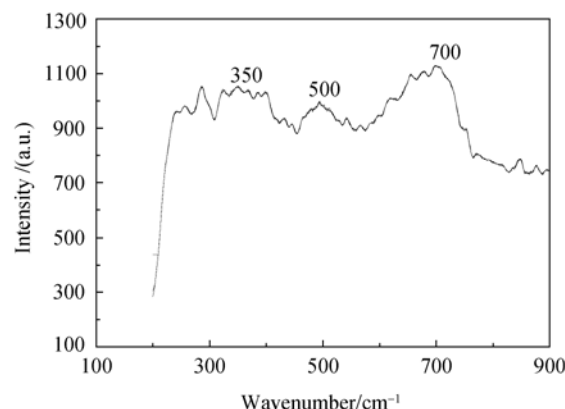


Fig. 2 Raman spectrum of sample S3

The size, morphology and agglomeration state of samples S1, S3 and S4 were investigated by HRTEM, as shown in Fig. 3. Figure 3(a) reveals that S1 exhibits the three dimensional fractal formed by poor-crystallized nanoparticle agglomeration, typical morphology of products derived from the conventional combustion method<sup>[29]</sup>. Fig. 3(b) shows well-dispersed cubic  $\gamma$ -Fe<sub>2</sub>O<sub>3</sub> nanoparticles of S3 with a size of 25 nm, indicating that the introduction of KCl into the solution combustion synthesis process can break up three-dimensional network and disintegrate the agglomerates of nanoparticles, resulting in well dispersed nanoparticles. Furthermore, S3 is highly crystallized, as can be seen from Fig. 3(b), which is in accordance with the XRD results (Fig. 1 (c)). Fig. 3(c) shows heterogeneous crystals with particle sizes of 20–80 nm, referring to mixing-phase Fe<sub>2</sub>O<sub>3</sub> for S4. The above results indicate that the KCl/NO<sub>3</sub><sup>-</sup> molar ratio has strong influence on the size, morphology and dispersion of Fe<sub>2</sub>O<sub>3</sub> nanoparticles. The BET surface areas of S1, S3 and S4 are 21.96, 102.35 and 32.36 m<sup>2</sup>/g, respectively. It is clear that the pure  $\gamma$ -Fe<sub>2</sub>O<sub>3</sub> nanoparticles (S3) exhibit the highest specific surface area, which may be mainly due to the smaller size and better dispersion. The specific surface area of S4 is less than that of S3, which may be caused by the formation of mixed-phase Fe<sub>2</sub>O<sub>3</sub> with a wide size distribution.

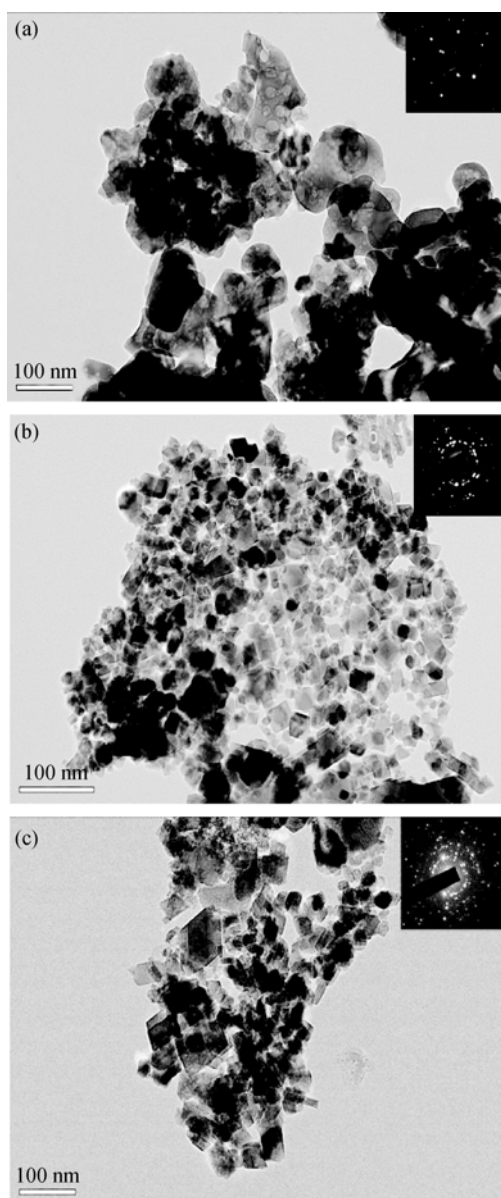


Fig. 3 HRTEM images of sample (a) S1, (b) S3 and (c) S4

In order to further explore the effect of KCl on the crystal-phase and dispersion of the obtained  $\text{Fe}_2\text{O}_3$ , TG-DTA of the gel precursors of non-salt gel (S1) and salt-assisted gel (S3) are measured and the results are shown in Fig.4. It can be seen from Fig.4 that introduction of KCl lowers the peak temperature of decomposition of the gels from  $437^\circ\text{C}$  to  $412^\circ\text{C}$  and the weight loss happens in the narrower temperature regions ( $300\text{--}420^\circ\text{C}$ ) for the S3 gel than that for S1 gel ( $180\text{--}440^\circ\text{C}$ ), which indicates that the introduction of KCl inhibit the combustion reaction at lower temperature and make the reaction happen at a short time. In the combustion process, the large amount of heat has been released owing to the redox of oxidant and fuel. For salt-assisted gel precursors (S3), the release large

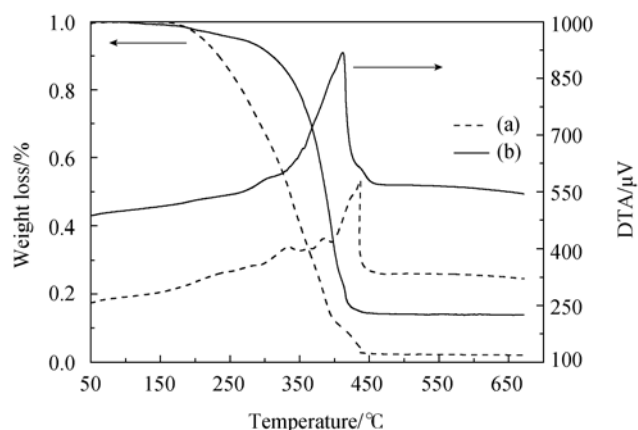


Fig. 4 TG and DTA curves of the gel precursors of sample S1 (a) and S3 (b)

amount of heat in the very short time result in instant high temperature of the reaction system and the salt precipitation *in situ* is completed in an instant to form a thin layer of salt crust on the surface of the newly formed nanoparticles<sup>[30]</sup>. After the rapid cooling, the salt-coated  $\gamma\text{-Fe}_2\text{O}_3$  nanoparticles are trapped into the salt matrix, since the frozen salt matrix is no longer able to move, which prevents the re-agglomeration of the newly formed crystallites and stabilizes the derived nanoparticles<sup>[31]</sup>. Followed by removing the soluble salt by aqueous wash and drying, the well-dispersed  $\gamma\text{-Fe}_2\text{O}_3$  nanoparticles can be obtained.

It is also noted that some KCl was observed to be separated from the whole reaction system during the preparation processing of S4 and S5. The separation of KCl might decrease the uniformity of inner reaction system and transform some  $\gamma\text{-Fe}_2\text{O}_3$  nanoparticles to  $\alpha\text{-Fe}_2\text{O}_3$ . However, the exact reason of the formation of mixed crystal phase of  $\alpha\text{-Fe}_2\text{O}_3$  and  $\gamma\text{-Fe}_2\text{O}_3$  needs to be further studied.

### 3 Conclusions

In this work,  $\text{Fe}_2\text{O}_3$  nanoparticles with different crystal phases were prepared by a simple salt-assisted combustion method. The  $\text{KCl}/\text{NO}_3^-$  molar ratio is a key factor in the formation of  $\text{Fe}_2\text{O}_3$  with different crystal phases. As-prepared  $\alpha\text{-Fe}_2\text{O}_3$  formed without addition of KCl exhibits a typical morphology of combustion product with agglomeration and small specific surface area. Well-dispersed  $\gamma\text{-Fe}_2\text{O}_3$  nanoparticles with a narrow size distribution can be formed when the  $\text{KCl}/\text{NO}_3^-$  molar ratio is 1:1. Further increase the  $\text{KCl}/\text{NO}_3^-$  molar ratio to 2:1 results in formation of the mixed  $\alpha\text{-Fe}_2\text{O}_3$  and  $\gamma\text{-Fe}_2\text{O}_3$  nanoparticles with a wide size distribution. The presence of KCl is found to result in increase in the specific surface area of the products from  $21.96$  to  $102.35\text{ m}^2/\text{g}$ .

## References:

- [1] ZHENG Yuan-hui, CHENG Yao, WANG Yuan-sheng, *et al.* Quasicubic  $\alpha$ -Fe<sub>2</sub>O<sub>3</sub> nanoparticles with excellent catalytic performance. *The Journal of Physical Chemistry B*, 2006, **110**(7): 3093–3097.
- [2] Bailey J K, Brinker C J, McCartney M L. Growth mechanisms of iron oxide particles of differing morphologies from the forced hydrolysis of ferric chloride solutions. *Journal of Colloid and Interface Science*, 1993, **157**(1): 1–13.
- [3] Hamada S, Matijević E. Preparation of uniform cubic hematite particles by hydrolysis of ferric chloride in alcohol-water solutions. *Journal of Colloid and Interface Science*, 1981, **84**(1): 274–277.
- [4] Hamada S, Matijević E. Formation of monodispersed colloidal cubic hematite particles in ethanol + water solutions. *Journal of the Chemical Society. Faraday Transactions*, 1982, **178**: 2147–2156.
- [5] Ozaki M, Kratochvil S, Matijević E. Formation of monodispersed spindle-type hematite particles. *Journal of Colloid and Interface Science*, 1984, **102**(1): 146–151.
- [6] Park G S, Shino D, Waseda Y, *et al.* Internal structure analysis of monodispersed pseudocubic hematite particles by electron microscopy. *Journal of Colloid and Interface Science*, 1996, **177**(1): 198–207.
- [7] Sugimoto T, Muramatsu A, Sakata K, *et al.* Characterization of hematite particles of different shapes. *Journal of Colloid and Interface Science*, 1993, **158**(2): 420–428.
- [8] Sugimoto T, Sakata K. Preparation of monodisperse pseudocubic  $\alpha$ -Fe<sub>2</sub>O<sub>3</sub> particles from condensed ferric hydroxide gel. *Journal of Colloid and Interface Science*, 1992, **152**(2): 587–590.
- [9] Sugimoto T, Sakata K, Muramatsu A. Formation mechanism of monodisperse pseudocubic  $\alpha$ -Fe<sub>2</sub>O<sub>3</sub> particles from condensed ferric hydroxide gel. *Journal of Colloid and Interface Science*, 1993, **159**(2): 372–382.
- [10] KAN Shi-hai, YU San, PENG Xiao-gang, *et al.* Formation process of nanometer-sized cubic ferric oxide single crystals. *Journal of Colloid and Interface Science*, 1996, **178**(2): 673–680.
- [11] KAN Shi-hai, ZHANG Xin-tong, YU San, *et al.* Synthesis of uniform ferric oxide particles from deionized colloids. *Journal of Colloid and Interface Science*, 1997, **191**(2): 503–509.
- [12] Kandori K, Ishikawa T. TPD-MS-TG study of hematite particles produced by the forced hydrolysis reaction. *Physical Chemistry Chemical Physics*, 2001(3): 2949–2954.
- [13] Kandori K, Okamoto N, Ishikawa T. Preparation of nanoporous micrometer-scale hematite particles by a forced hydrolysis reaction in the presence of polyethylene glycol. *Langmuir*, 2002, **18**(7): 2895–2900.
- [14] Kandori K, Ishikawa T. Preparation and microstructural studies on hydrothermally prepared hematite. *Journal of Colloid and Interface Science*, 2004, **272**(1): 246–248.
- [15] Konishi Y, Kawamura T, Asai S. Microstructural and magnetic studies on hydrothermally prepared hematite. *Metallurgical and Materials Transactions B*, 1994, **25**(2): 165–170.
- [16] Sahu K K, Rath C, Mishra N C, *et al.* Microstructural and magnetic studies on hydrothermally prepared hematite. *Journal of Colloid and Interface Science*, 1997, **185**(2): 402–410.
- [17] SHANG Yu-xing, Weert G V. Iron control in nitrate hydrometallurgy by autoclave hydrolysis of iron (III) nitrate. *Hydrometallurgy*, 1993, **33**(3): 273–290.
- [18] Hiroshi Shiho, Nobuo Kawahashi. Iron compounds as coatings on polystyrene latex and as hollow spheres. *Journal of Colloid and Interface Science*, 2000, **226**(1): 91–97.
- [19] MA Zhen-ye, LI Feng-sheng, CUI Ping, *et al.* Preparation of nanometer-sized Fe<sub>2</sub>O<sub>3</sub> and its catalytic performance for ammonium perchlorate decomposition. *Chinese Journal of Catalysis*, 2003, **24**(10): 795–798. (In Chinese)
- [20] Basavaraja S, Vijayanand H, Venkataraman A. Characterization of  $\gamma$ -Fe<sub>2</sub>O<sub>3</sub> nanoparticles synthesized through self-propagating combustion route. *Synthesis and Reactivity in Inorganic, Metal-Organic, and Nano-Metal Chemistry*, 2007, **37**(6): 409–412.
- [21] CHEN Wei-Fan, LI Feng-Sheng, YU Ji-Yi. Combustion synthesis and characterization of nanocrystalline CeO<sub>2</sub>-based powders via ethylene glycol-nitrate process. *Materials Letters*, 2006, **60**(1): 57–62.
- [22] Chick L A, Maupin G D, Pederson L R. Glycine-nitrate synthesis of a ceramic-metal composite. *Nanostructured Materials*, 1994, **4**(5): 603–615.
- [23] CHEN Wei-Fan, LI Feng-Sheng, YU Ji-Yi, *et al.* Novel salt-assisted combustion synthesis of high surface area ceria nanopowders by an ethylene glycol-nitrate combustion process. *Journal of Rare Earths*, 2006, **24**(4): 434–439.
- [24] JIAO Huan, WEI Ling-qi, ZHANG Na, *et al.* Melting salt assisted sol-gel synthesis of blue phosphor Y<sub>2</sub>SiO<sub>5</sub>: Ce. *Journal of the European Ceramic Society*, 2007, **27**(1): 185–189.
- [25] LI Li, SHI Li-yi, CAO Shao-mei, *et al.* LiNO<sub>3</sub> molten salt assisted synthesis of spherical nano-sized YSZ powders in a reverse micro-emulsion system. *Materials Letters*, 2008, **62**(12/13): 1909–1912.
- [26] ZHANG Xiao-juan, JIANG Wei, SONG Dan, *et al.* Salt-assisted combustion synthesis of highly dispersed super paramagnetic CoFe<sub>2</sub>O<sub>4</sub> nanoparticles. *Journal of Alloys and Compounds*, 2009, **475**(1/2): L34–L37.
- [27] Varadwaj K S K, Panigrahi M K, Ghose J. Effect of capping and particle size on Raman laser-induced degradation of  $\gamma$ -Fe<sub>2</sub>O<sub>3</sub> nanoparticles. *Journal of Solid State Chemistry*, 2004, **117**(11): 4286–4292.
- [28] Xia B, Lenggoro I W, Okuyama K. Novel route to nanoparticle synthesis by salt-assisted aerosol decomposition. *Advanced Materials*, 2001, **13**(20): 1579–1582.
- [29] Sena D, Deb P, Mazumder S, *et al.* Microstructural investigations of ferrite nanoparticles prepared by non-aqueous precipitation route. *Materials Research Bulletin*, 2000, **35**(8): 1243–1250.
- [30] CHEN Wei-fan, LI Feng-sheng, Yu Ji-yi, *et al.* Rapid synthesis of mesoporous ceria–zirconia solid solutions via a novel salt-assisted combustion process. *Materials Research Bulletin*, 2006, **41**(12): 2318–2324.
- [31] LI Yong-xiu, CHEN Wei-fan, ZHOU Xue-zhen, *et al.* Synthesis of CeO<sub>2</sub> nanoparticles by mechanochemical processing and the inhibiting action of NaCl on particle agglomeration. *Materials Letters*, 2005, **59**(1): 48–52.

## 不同晶态纳米 $\text{Fe}_2\text{O}_3$ 的盐控合成

宋 军<sup>1</sup>, 马振叶<sup>1,2</sup>, 李 成<sup>1</sup>, 吴如军<sup>2</sup>

(1. 南京工业大学 材料化学工程国家重点实验室, 南京 210009; 2. 南京师范大学 化学与环境科学学院, 南京 210097)

**摘 要:** 以  $\text{Fe}(\text{NO}_3)_3 \cdot 9\text{H}_2\text{O}$  为氧化剂, 聚乙二醇(PEG2000)为燃料, 采用 KCl 盐助燃烧法制备了不同晶态的纳米  $\text{Fe}_2\text{O}_3$  粒子, 并用 HRTEM、XRD、LRS 和 BET 对其形貌和结构进行了表征. 结果表明, 纳米  $\text{Fe}_2\text{O}_3$  的晶态(包括纯  $\alpha\text{-Fe}_2\text{O}_3$ 、纯  $\gamma\text{-Fe}_2\text{O}_3$  以及  $\alpha\text{-Fe}_2\text{O}_3$  和  $\gamma\text{-Fe}_2\text{O}_3$  混晶)可以通过调整  $\text{KCl}/\text{NO}_3^-$  的摩尔比来控制合成. 将惰性盐 KCl 引入到燃烧反应中, 可以制得粒径小、比表面大、均匀分散的  $\gamma\text{-Fe}_2\text{O}_3$  纳米粒子. 另外, 本实验也探索了惰性盐 KCl 的作用机理.

**关 键 词:** 纳米  $\text{Fe}_2\text{O}_3$ ; 盐助燃烧法; 晶态

中图分类号: TQ138

文献标识码: A